

# 1 Access to Ordered Porous Molybdenum Oxycarbide/Carbon 2 Nanocomposites\*\*

3 *Thomas Lunkenbein, Dirk Rosenthal, Torsten Otremba, Frank Girgsdies, Zihui Li, Hiroaki Sai,*  
4 *Carina Bojer, Gudrun Auffermann, Ulrich Wiesner, and Josef Breu\**

5

Heterogeneous catalysis is still dominated by metals, metal oxides, and metal sulfides.<sup>[1]</sup> However, additional demands for more sophisticated, efficient, and economical processes require alternative catalytic materials. For instance, in industrial catalytic processes there is a growing interest in substituting rare and expensive noble metal catalysts by cheap and abundant transition metal carbide (TC)

materials. For this reason, TCs have attracted considerable interest in current academic catalysis research. It has e.g. been demonstrated by Levy and Boudart that the combination of group VI transition metals and carbon can result in Pt-like properties with respect to activity, selectivity, and resistance against poisoning.<sup>[1,2]</sup> In particular, in catalytic reactions involving the transformation of C-H bonds of hydrocarbons, i.e. dehydrogenation, hydrogenation, and hydrogenolysis, TCs received a great deal of attention.<sup>[3]</sup>

[\*] Dipl. Chem. Thomas Lunkenbein, B. Sc. Carina Bojer, Prof. Dr. Josef Breu  
Anorganische Chemie I  
Universität Bayreuth  
Universitätsstraße 30, 95440 Bayreuth, Germany  
Fax: +49 921 55 2788  
E-mail: josef.breu@uni-bayreuth.de  
Homepage: <http://www.ac1.uni-bayreuth.de>

Applying conventional carburization methods, porous TCs with high specific surface areas are difficult to obtain. Standard metallurgy approaches involve reaction of the metals with carbon at temperatures above 1200 °C.<sup>[4]</sup> This inevitably yields bulk TCs with low surface area and mediocre catalytic activity. Exploration of the true potential of TCs requires the development of appropriate synthesis techniques leading to TCs with nanoscale particle size, high surface area, large pore volumes.<sup>[5]</sup> Further studies on the accessibility of the active sites by CO chemisorption experiments reveal an CO uptake between 178 and 950 μmol/g.<sup>[6]</sup> High surface area TCs have been reported using a temperature programmed reduction,<sup>[6]</sup> high-temperature decomposition,<sup>[7]</sup> or carbothermal reduction.<sup>[8]</sup> Although these preparation methods deliver high surface area and catalytically active TCs,<sup>[9]</sup> the resulting carbides do not feature ordered and uniform pores that might optimize mass transport.<sup>[10]</sup>

Dr. Dirk Rosenthal, Dr. Frank Girgsdies  
Anorganische Chemie  
Fritz-Haber-Institut der Max-Planck-Gesellschaft  
Faradayweg 3-6, 14195 Berlin, Germany

Zihui Li, Hiroaki Sai, Prof. Dr. Ulrich Wiesner  
Materials Science & Engineering  
Cornell University  
Ithaca, NY 14853, USA

Torsten Otremba  
Institut für Chemie  
Technische Universität Berlin  
Straße des 17. Juni 124  
10623 Berlin, Germany

Dr. Gudrun Auffermann  
Max-Planck Institut für Chemische Physik fester Stoffe  
Nöthnitzer Str. 40  
01187 Dresden

Techniques for organizing TCs on the mesoscale using inorganic or organic matrices are scarce. Ordered mesoporous TCs have been reported by exotemplating of polyoxometalates into mesoporous silica followed by carburization using an additional carbon source like CO or CH<sub>4</sub>.<sup>[11]</sup> Ordered micro-/mesoporous TC/carbon (TC/C) nanocomposites with pore volumes of 0.43–0.49 cm<sup>3</sup> g<sup>-1</sup> were synthesized by endotemplating of pre-synthesized, stabilized TOx nanoparticle suspensions into a pluronic template followed by carbothermal reduction.<sup>[12]</sup> For successful carburization additional carbon sources and/or curing steps were required rendering the process rather complex.

[\*\*] This work was supported by the Deutsche Forschungsgemeinschaft (DFG) within the Collaborative Research Center (SFB) 840 (Project A7). T. L. acknowledges the international graduate school of the ENB "Structures, Reactivity and Properties of Metal Oxides" for a fellowship. Z. L. was supported by the U.S. Department of Homeland Security under Cooperative Agreement Number 2009-ST-108-LR0004. H.S. was supported through the National Science Foundation (NSF) grant DMR-1120296. The X-ray equipment was supported by Department of Energy grant DEFG-02-97ER62443. CHESS was supported by the NSF and NIH-NIGMS via DMR-0225180. We thank Prof. Sol Gruner (Department of Physics, Cornell University) for letting us acquire some of the SAXS patterns in his lab. Prof. Dr. Rüdiger Kniep is gratefully acknowledged for the support with elemental analysis. We also thank Prof. Dr. Axel H. E. Müller for ensuring easy access to its anionic polymerization reactors. Dr. Andrey Tarasov is acknowledged for thermogravimetric measurements. Klaus Friedel-Ortega, Dr. Annette Trunschke and Prof. Dr. Robert Schlögl are acknowledged for fruitful discussions and supporting with heat treatment and TEM equipment.

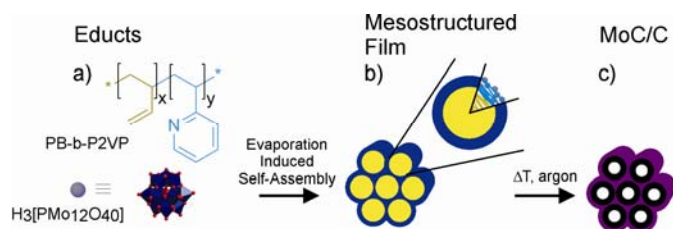
Aside from catalysis, such hierarchical porous TC/C nanocomposites (micropores in the wall of mesopores) have been shown to be excellent precursors for super capacitors.<sup>[12d]</sup> In brief, ordered mesoporous channels support penetration and transport of the electrolyte. The open space is an essential feature for highly efficient capacitors. Simultaneously, micropores embedded in the walls of mesopores provide additional space for charge storage.<sup>[13]</sup>

TC/C nanocomposites are, however, not only superior to pure TCs in super capacitor applications, their catalytic activity and stability is also advanced.<sup>[14]</sup> The development of a general method for direct access to ordered mesoporous TC/C nanocomposites with TC walls, uniform and accessible pores, and high porosity is consequently highly desirable.

Here we describe a direct route towards hexagonally ordered mesoporous molybdenum carbide/carbon (MoC/C) nanocomposites by endotemplating followed by subsequent carbothermal reduction in inert atmosphere. Molybdophosphoric acid (H<sub>3</sub>PMo<sub>12</sub>O<sub>40</sub>;

H<sub>3</sub>PMo) was adopted as molybdenum precursor. A structure directing agent (SDA) particularly rich in sp<sup>2</sup>-carbon was applied poly(butadiene-*block*-2-vinylpyridine) (PB-*b*-P2VP), which at the same time served as carbon source in the carburization reaction. As we will show, key to successful generation of mesoporous materials without loss of the block copolymer directed mesostructure was heat treatment of the as-made composites to temperatures above 700 °C.

Scheme 1 summarizes our approach.



**Scheme 1.** Illustration of the synthesis scheme of MoC/C: a) Chemical structure of PB-*b*-P2VP (top) and H<sub>3</sub>PMo (bottom). The indices *x* and *y* denote the degrees of polymerization (DP) of the PB (*x*=411) and P2VP units (*y*=75). b) Inverse hexagonal mesophase obtained after solvent evaporation. c) MoC/C with retained mesostructure after heat treatment (740 °C) in argon atmosphere.

After synthesis of the block copolymer PB-*b*-P2VP (30 kg/mol, 26wt% P2VP, PDI of 1.02) and composites (see Supporting Information for details) structural assignment of the resulting mesostructured PB-*b*-P2VP/H<sub>3</sub>PMo nanocomposites was accomplished by SAXS measurements (Figure 1). In Figure 1a the expected peak positions for higher order Bragg reflections of a hexagonal lattice centred around the first order maximum at angular positions equal to the ratio of 1:√3:2:√7:3:√12:√13 are indicated by vertical ticks and suggest a morphology of hexagonally ordered cylinders. The corresponding spacing (*d*-spacing) is 39 nm. A hexagonal mesostructure was further corroborated by brightfield TEM measurements (Figure 2a,b). The TEM images evidence the inverse hexagonal mesostructure of the PB-*b*-P2VP/H<sub>3</sub>PMo nanocomposite with a PB pore diameter of 27.0 ± 1.6 nm and a wall thickness of 9.0 ± 1.1 nm. The high resolution (HR)-TEM image in Figure 2b shows the good dispersion of discrete H<sub>3</sub>PMo units selectively incorporated into the P2VP walls. The diameter of the monodisperse dark dots was estimated to be 1.2 nm, consistent with the reported diameter of H<sub>3</sub>PMo clusters (1.1 nm).<sup>[15]</sup> The good dispersion of the H<sub>3</sub>PMo units within the polymeric matrix was further corroborated by the amorphous nature of the powder patterns of as-synthesized PB-*b*-P2VP/H<sub>3</sub>PMo nanocomposites (Figure SI 3b).

The catalytic functionality of such hexagonal ordered PB-*b*-P2VP/H<sub>3</sub>PMo nanocomposites can only be achieved if the material can be rendered into mesoporous POM with retaining the mesostructure. However, complete removal of the polymeric matrix resulting in pure mesoporous Keggin-Type polyoxometalates (Keggin POM) unfortunately is not straight forward for the following reasons: It is well established that unlike rutile nanocrystals, Keggin POMs show almost no tendency to connect covalently to neighbouring units by condensation of two hydroxyl groups since the most basic oxygens are the bridging ones which are remote from the surface of the cluster. Thus a rigid inorganic framework that prevents the mesostructure to collapse cannot be constructed during pyrolysis of the composite films. Applying isopoly acids of molybdenum does not solve the problem either: Vapour-phase sintering readily leads to micrometer-sized MoO<sub>3</sub>

crystals even at relative moderate temperatures and the mesostructure is lost. In any case the preparation of ordered and mesoporous molybdenum compounds is not trivial.

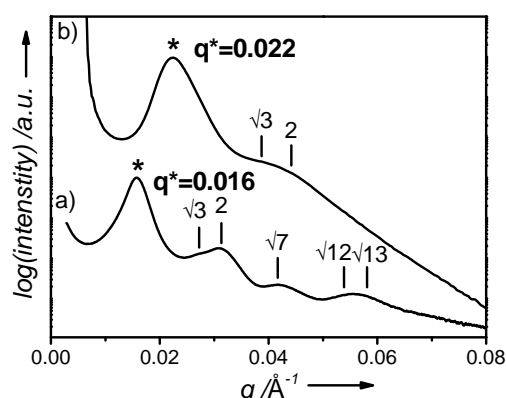


**Figure 1.** SAXS patterns of (a) as-synthesized PB-*b*-P2VP/H<sub>3</sub>PMo nanocomposite and (b) MoC/C. Expected peak positions for hexagonal lattices are indicated by vertical lines.

In line with these considerations, original efforts to generate mesoporous materials by heating below 700 °C failed. **More precise our experiments showed that below this temperature the *in-situ* formed rigid carbon hampers access to mesopores.** It was not until we went to higher temperatures that as-made composites could be converted to mesoporous materials without loss of the mesostructure. To understand and explain the chemical reactions involved upon heat treatment and to verify a mesoporous material we examined the mesostructured PB-*b*-P2VP/H<sub>3</sub>PMo nanocomposites in more detail conducting thermogravimetric analysis coupled with mass spectrometry (TGA-MS) in He atmosphere (Figure SI 4). TG-measurements showed an almost continuous mass loss below 700 °C, whereas above 700 °C a steep decay in the TG signal of 17 wt % was observed. The mass loss below 700 °C could be attributed to the pyrolysis of the diblock copolymer and the formation of the rigid carbon scaffold.<sup>[16]</sup> Above 700 °C the MS analysis showed the release of CO<sub>2</sub> and CO indicating the reduction of the molybdenum oxide species by parts of the carbonaceous material to carbides.<sup>[4]</sup>

During this heat treatment several processes occur: The sp<sup>2</sup> hybridized carbon is converted into a rigid carbonaceous scaffold; the H<sub>3</sub>PMo clusters decompose and parts of the carbonaceous material react with the molybdenum centres to form molybdenum carbides.

To generate mesoporous materials the as-synthesized inverse hexagonal PB-*b*-P2VP/H<sub>3</sub>PMo nanocomposites were heat treated under argon atmosphere in a tube furnace. Here we report on results taking composites that have been heated to 740 °C. As we will show, at this temperature the *in-situ* formed carbide nanocrystals arrange into a woven microstructure that together with the remaining rigid carbon scaffold assures the retention of the hexagonal mesostructure.

Structural characterization of the resulting MoC/C nanocomposites revealed preservation of the ordered mesostructure. SAXS patterns (Figure 1b) of heat-treated composites show a first-order maximum with corresponding *d*-spacing of 28.6 nm and a broader higher order reflex indicating some degree of long-range order. Expected higher order reflections for a hexagonal lattice at angular

position of  $\sqrt{3}$  and 2 of the first-order maximum are indicated via ticks above the broad scattering feature in Figure 1b. Assuming a hexagonal lattice the shift of the primary  $10$  reflection to higher  $q$  values implies a decrease of the cell dimension of 28 %. The structural assignment to a hexagonal lattice was corroborated by TEM studies (Figure 2c-f).

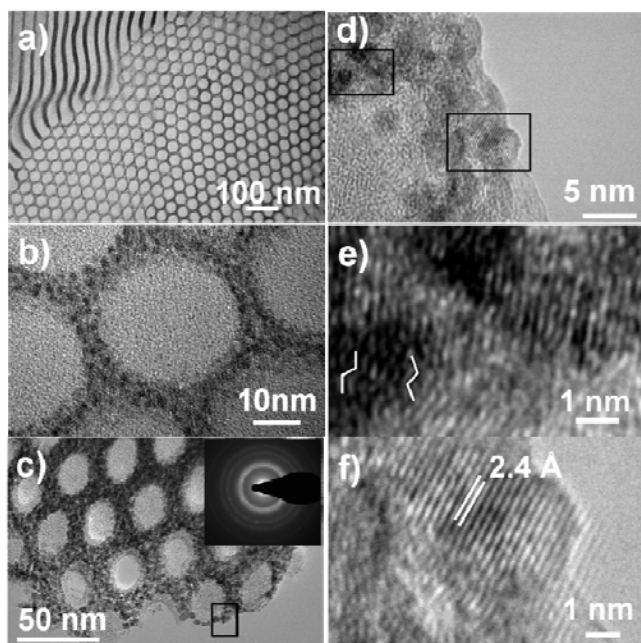


**Figure 2.** Representative bright-field TEM images of PB-b-P2VP/H<sub>3</sub>PMo nanocomposite (a and b) and of MoC/C at different magnifications (c-f). The inset in (c) represents a SAED pattern indicative for nanocrystalline MoO<sub>x</sub>C<sub>y</sub>. (d) is zooming in on the area in the black box in (c). The black boxes in (d) denote selected areas of which HR-TEM images (e, top, and f, bottom) were taken. (e) displays the chevron-like structure of MoO<sub>x</sub>C<sub>y</sub> along the [010] zone axis. f) shows a HR-TEM image of a single nanocrystal. The spacing of 2.4 Å is consistent with the (111) plane of MoO<sub>x</sub>C<sub>y</sub>.

TEM micrographs of MoC/C exhibit a well-defined 2D hexagonal mesostructure (Figure 2c) with pore diameters of  $19.3 \pm 4.0$  nm and wall thicknesses of  $13.1 \pm 1.6$  nm consistent with the observed d-spacing of the SAXS patterns (28.6 nm). TEM images also revealed the presence of narrowly size distributed carbide nanoparticles well dispersed in the carbon matrix and exhibiting an average diameter of roughly 4 nm. During heat treatment the randomly distributed H<sub>3</sub>PMo units within the P2VP matrix produced a large number of carbide nuclei leading to a rather small particle size. The *in-situ* formed rigid carbon scaffold capable of preventing collapse of the mesostructures upon heat treatment and carbide formation can clearly be identified around the pores in TEM (Figure SI 5).

Powder X-ray diffraction (PXRD) patterns of the heat-treated nanocomposites showed two broad reflections at angular positions of 37° and 43° (Figure SI 3c, Figure SI 6aA) attributed to the (111) and (200) planes of a face centred cubic (fcc) arrangement of MoC<sub>1-x</sub> or molybdenum oxycarbide (MoO<sub>x</sub>C<sub>y</sub>). The diffusive selected area electron diffraction pattern (SAED, inset: Figure 2c) further corroborated the formation of fcc-type carbide species. It has recently been highlighted that oxycarbides and fcc-MoC<sub>1-x</sub> possess similar PXRD patterns.<sup>[17]</sup> Figure 2f shows a HR-TEM image of a single nanocrystal. The spacing of 2.4 Å corresponds well with the

(111) plane of both, MoC<sub>1-x</sub> or MoO<sub>x</sub>C<sub>y</sub>. In order to clarify the nature of the carbide phase a combined analytical sequence of EA, TGA-MS in a hydrogen argon mixture (95/5 v/v), and HR-TEM measurements of MoC/C were conducted. The presence of considerable amounts of oxygen (EA, Table S1) and the concomitant release of CO and CH<sub>4</sub> in the TGA (additional weight loss of 6 wt %) as detected by MS profiles (Figure SI 7) were more in line with an oxycarbide species. In addition, HR-TEM images showed a chevron-like structure (Figure 2e). This structure is well known to result from atom vacancies in the [010] zone axis of crystalline MoO<sub>x</sub>C<sub>y</sub>.<sup>[18]</sup>

Nitrogen physisorption measurements (Figure 3a) of porous MoC/C exhibited a type I isotherm with a type H4 hysteresis. The specific surface area of 133 m<sup>2</sup>/g was determined by applying the BET equation. Since micropores were detected, the recommendations of Rouquerol *et al.* were followed for calculating the BET surface area.<sup>[19]</sup> Non-local density functional theory (NLDFT, slit/cylindrical pore kernel) was adopted to determine the pore size distribution and pore volumes. NLDFT analysis of nitrogen physisorption isotherms showed the presence of both, micro- and mesopores in MoC/C (Figure 3b). The estimated cumulative pore volume was 0.085 cm<sup>3</sup>/g. Approximately half of the total volume, 0.043 cm<sup>3</sup>/g, could be attributed to micropores (Figure SI 8). Four peaks at diameters of 0.68 nm, 1.27 nm, 3.79 nm, and 5.30 nm, were observed. Most likely, the micropore peaks are related to holes in the carbon scaffold. On first sight, the TEM images might suggest a rather uniform pore size of mesopores in the range of 19.3 nm. The pore size distribution, however, rapidly decayed after 5.3 nm. Only very little pore volume stretches the range up to a maximum of 17.5 nm. In agreement with TEM observation (Figure 2c and Figure SI 5) a rigid amorphous carbon scaffold lines the pores resulting in the size limitation and partial blocking of the voids. The hierarchical pore structure in which micropores are incorporated into the walls of ordered mesopores provided high specific surface area.

To further proof the concept of rigid carbon lining the pores, Raman spectroscopy was performed (Figure SI 9). The rigid carbon scaffold not only embedded the large number of MoO<sub>x</sub>C<sub>y</sub> nanocrystals, but also retained the hexagonal order of the mesopores. However, it also passivated the molybdenum oxycarbide centers by acting as a barrier to accessing reactive sites as shown by chemisorption experiments (Figure 3c). When MoC/C was pre-treated in He atmosphere no CO uptake was detectable (Figure 3c, squares). However, prior exposure of the composite to pure hydrogen atmosphere at 450 °C (Figure 3d, circles) and 600 °C (Figure 3c, triangles) led to an irreversible CO uptake of 84 μmol/g and 165 μmol/g, respectively. Hydrogenation and removal of carbon that covered the surface may facilitate diffusion of CO molecules and allow adsorption. Thus, H<sub>2</sub> pre-treatment resulted in the modification of the chemisorption properties of the material that may be caused by partial reduction of the oxycarbide surface under formation of Mo<sub>2</sub>C (Figure SI 6aB) and changes in the pore geometry (Figure SI 10).

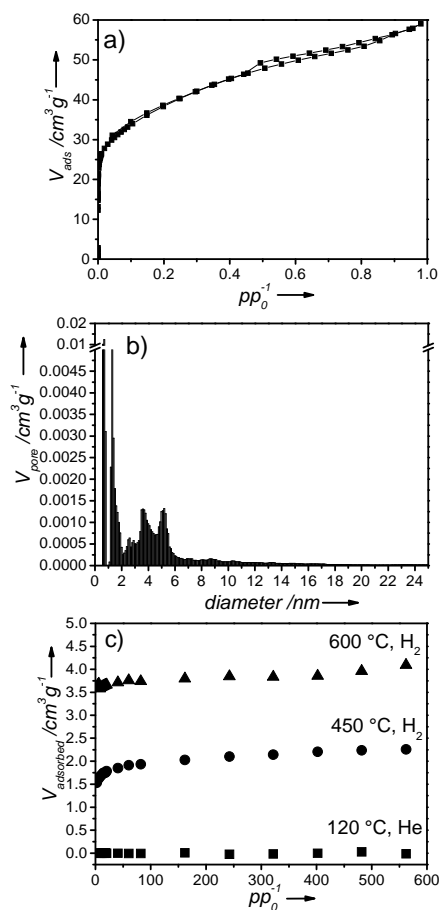


**Figure 3.** a) Nitrogen physisorption isotherm of MoC/C. b) NLDFT analysis of nitrogen adsorption isotherms of the micropore and mesopore distribution of MoC/C. c) Chemisorption curves for the irreversible CO uptake of MoC/C after different pre-treatments: in He atmosphere at 120 °C (squares), in pure H<sub>2</sub> atmosphere at 450 °C (circles) and in pure H<sub>2</sub> atmosphere at 600 °C (triangles). In all cases holding times were 2h.

The hexagonal mesostructure was maintained as evidenced by TEM investigations (Figure SI 6b). Hence, appropriate pre-treatment in reductive atmosphere could enable a way to uncover carbide centres activating the material for catalysis. To proof this hypothesis activated MoC/C was tested as potential catalyst in the decomposition of NH<sub>3</sub>. Preliminary investigations revealed activity of MoC/C in the decomposition reaction of NH<sub>3</sub> (Figure SI 11). The activation energy was estimated to be 155 kJ/mol (Figure SI 11b) which is in close agreement with results reported earlier for other molybdenum carbides (151 kJ/mol).<sup>[20]</sup>

In summary, we have established a direct path to mesoporous MoC/C nanocomposites by simple high temperature (>700 °C) heat treatment of a hexagonally ordered diblock copolymer/heteropoly acid nanocomposite in argon atmosphere. The diblock copolymer served multiple tasks, i.e. as SDA and as carbon source. The H<sub>3</sub>PMo units could easily be converted into MoO<sub>x</sub>C<sub>y</sub> nanoparticles that were embedded in a porous carbon matrix. The resulting MoC/C nanocomposites exhibited inverse hexagonal order, hierarchical pore structure, and high surface area. These MoO<sub>x</sub>C<sub>y</sub> nanoparticles could be activated by uncovering them via pre-treatment in H<sub>2</sub>. MoC/C nanocomposites showed not only activity in catalysis, such as NH<sub>3</sub>

decomposition, but the hierarchical pore structure may also render them interesting for super capacitor applications.

Received: ((will be filled in by the editorial staff))

Published online on ((will be filled in by the editorial staff))

**Keywords:** polyoxometalate · carbides · self-assembly · heterogeneous catalysis · physisorption

- [1] A. M. Alexander, J. S. J. Hargreaves, *Chem. Soc. Rev.* **2010**, 39.
- [2] R. B. Levy, M. Boudart, *Science* **1973**, 181, 547-549.
- [3] a) H. H. Hwu, J. G. Chen, *Chem. Rev.* **2004**, 105, 185-212; b) J. G. Chen, *Chem. Rev.* **1996**, 96, 1477-1498.
- [4] A. Hanif, T. Xiao, A. P. E. York, J. Sloan, M. L. H. Green, *Chem. Mater.* **2002**, 14, 1009-1015.
- [5] C. Giordano, C. Erpen, W. Yao, M. Antonietti, *Nano Lett.* **2008**, 8, 4659-4663.
- [6] a) J. S. Lee, S. T. Oyama, M. Boudart, *J. Catal.* **1987**, 106, 125-133, b) J.S. Lee, L. Volpe, F.H. Riberio, M. Boudart, *J. Catal.* **1989**, 112, 44-53.
- [7] H. Preiss, B. Meyer, C. Olschewski, *J. Mater. Sci.* **1998**, 33, 713-722.
- [8] a) M. J. Ledoux, S. Hantzer, C. P. Huu, J. Guille, M. P. Desaneaux, *J. Catal.* **1988**, 114, 176-185; b) D. Mordenti, D. Brodzki, G. Djega-Mariadassou, *J. Solid State Chem.* **1998**, 141, 114-120.
- [9] a) T. C. Xiao, A. P. E. York, V. C. Williams, H. Al Megren, A. Hanif, X. Y. Zhou, M. L. H. Green, *Chem. Mater.* **2000**, 12, 3896-3905; b) T. Xiao, H. Wang, J. Da, K. S. Coleman, M. L. H. Green, *J. Catal.* **2002**, 211, 183-191; c) M. A. Ecomier, K. Wilson, A. F. Lee, *J. Catal.* **2003**, 215, 57-65.
- [10] a) D. L. Li, H. S. Zhou, I. Honma, *Nature Mater.* **2004**, 3, 65-72; b) F. Hoffmann, M. Cornelius, J. Morell, M. Fröba, *Angew. Chem.* **2006**, 118, 3290-3328; *Angew. Chem. Int. Ed.* **2006**, 45, 3216-3251; c) M. C. Orilall, U. Wiesner, *Chem. Soc. Rev.* **2011**, 40, 520-535; d) F. Schüth, *Angew. Chem.* **2003**, 115, 3730-3750; *Angew. Chem. Int. Ed.* **2003**, 42, 3604-3622, e) M. Hartmann, *Angew. Chem.* **2004**, 116, 6004-6006; *Angew. Chem. Int. Ed.* **2004**, 43, 5880-5882.
- [11] a) X. Cui, H. Li, L. Guo, D. He, H. Chen, J. Shi, *Dalton Trans.* **2008**; b) Z. Wu, Y. Yang, D. Gu, Q. Li, D. Feng, Z. Chen, B. Tu, P. A. Webley, D. Zhao, *Small* **2009**, 5, 2738-2749.
- [12] a) J. Han, J. Duan, P. Chen, H. Lou, X. Zheng, H. Hong, *Chem. Sus. Chem* **2012**, 5, 727-733; b) C. H. Huang, D. Gu, D. Zhao, R. A. Doong, *Chem. Mater.* **2010**, 22, 1760-1767, c) T. Yu, Y. Deng, L. Wang, R. Liu, L. Zhang, B. Tu, D. Zhao, *Adv. Mater.* **2007**, 19, 2301-2306; d) H. J. Liu, J. Wang, C. X. Wang, Y. Y. Xia, *Adv. Energy Mater.* **2011**, 1, 1101-1108.
- [13] J. Chmiola, G. Yushin, Y. Gogotsi, C. Portet, P. Simon, P. L. Taberna, *Science* **2006**, 313, 1760-1763.
- [14] D. Mordenti, D. Brodzki, G. Djega-Mariadassou, *J. Solid State Chem.* **1998**, 141, 114-120.
- [15] A. Stein, M. Fendorf, T. P. Jarvie, K. T. Müller, A. J. Benesi, T. E. Mallouk, *Chem. Mater.* **1995**, 7, 304-313.
- [16] J. Lee, M. C. Orilall, S. C. Warren, M. Kamperman, F. J. Disalvo, U. Wiesner, *Nature Mater.* **2008**, 7, 222-228.
- [17] T. C. Xiao, A. P. E. York, V. C. Williams, H. Al Megren, A. Hanif, X. y. Zhou, M. L. H. Green, *Chem. Mater.* **2000**, 12, 3896-3905.
- [18] S. T. Oyama, C. Delporte, C. Pham-Huu, M. J. Ledoux, *Chem. Lett.* **1997**, 9, 949-950.
- [19] J. Rouquerol, P. Llewellyn, F. Rouquerol, in *Studies in Surface Science and Catalysis Characterization of Porous Solids VII Proceedings of the 7th International Symposium on the Characterization of Porous Solids (COPS-VII), Aix-en-Provence, France, 26-28 May 2005* Ed.: P. L. Llewellyn, Elsevier, **2007**, pp. 49-56.
- [20] C. Jeong-Gil, *J. Catal.* **1999**, 182, 104-116.

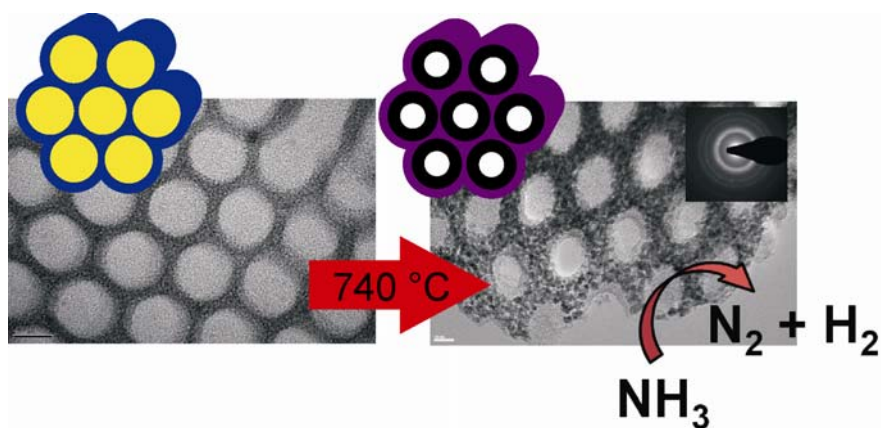


## Ordered Carbides

Thomas Lunkenbein, Dirk Rosenthal, Torsten Otremba, Frank Girgsdies, Zihui Li, Hiroaki Sai, Carina Bojer, Gudrun Auffermann, Ulrich Wiesner, and Josef Breu\*

Page – Page

Direct Access to Ordered Porous Molybdenum Oxycarbide/Carbon Nanocomposites



**Hexagonally ordered mesoporous molybdenum oxycarbide/carbon nanocomposites** (MoC/C) were directly accessed by heat treatment of mesostructured poly(butadiene-*block*-2-vinylpyridine) (PB-*b*-P2VP) and molybdophosphoric acid. PB-*b*-P2VP serves as structure directing agent and as carbon source in the carburization allowing the hybrids to be converted to MoC/C nanocomposites in one step. The *in-situ* formed carbon scaffold stabilized the hexagonal mesostructure and served as matrix for MoC nanocrystals (4 nm). The high specific surface area (133 m<sup>2</sup>g<sup>-1</sup>) obtained for MoC/C nanocomposites renders the materials interesting for potential applications as precursor for super capacitors. MoC/C showed promising results in the catalytic decomposition of NH<sub>3</sub>.

1

2